water

Article

Assessing Flood Risk: LH-Moments Method and Univariate Probability Distributions in Flood Frequency Analysis

Cornel Ilinca , Stefan Ciprian Stanca and Cristian Gabriel Anghel *

Faculty of Hydrotechnics, Technical University of Civil Engineering Bucharest, Lacul Tei nr.122-124, 020396 Bucharest, Romania; cornel@utcb.ro (C.I.); stefan-ciprian.stanca@phd.utcb.ro (S.C.S.)
* Correspondence: cristian.anghel@utcb.ro

Abstract: This study examines all of the equations necessary to derive the parameters for seven probability distributions of three parameters typically used in flood frequency research, namely the Pearson III (PE3), the generalized extreme value (GEV), the Weibull (W3), the log-normal (LN3), the generalized Pareto Type II (PG), the Rayleigh (RY) and the log-logistic (LL3) distributions, using the higher-order linear moments method (LH-moments). The analysis represents the expansion of previous research whose results were presented in previous materials, and is part of hydrological research aimed at developing a standard for calculating maximum flows based on L-moments and LH-moments. The given methods for calculating the parameters of the examined distributions are used to calculate the maximum flows on Romania's Prigor River. For both methods, the criterion for selecting the most suitable distribution is represented by the diagram of the L-skewness–L-kurtosis and LH-skewness–LH-kurtosis. The results for Prigor River show that the PG distribution is the best model for the L-moments method, the theoretical values of the statistical indicators being 0.399 and 0.221. The RY distribution is the best model for the LH-moments technique, with values of 0.398 and 0.192 for the two statistical indicators.

Keywords: parameters; frequency analysis; log-logistic; linear moments; Pareto; Rayleigh; separation effect; Weibull

Citation: Ilinca, C.; Stanca, S.C.; Anghel, C.G. Assessing Flood Risk: LH-Moments Method and Univariate Probability Distributions in Flood Frequency Analysis. *Water* **2023**, *15*, 3510. https://doi.org/10.3390/w15193510

Academic Editor: Athanasios Loukas

Received: 7 September 2023
Revised: 2 October 2023
Accepted: 7 October 2023
Published: 8 October 2023

1. Introduction and Background

Flood frequency analysis (FFA) is critical for identifying maximum flows that correspond to particular annual exceedance probabilities of interest. In Romania FFA plays a significant role in estimating maximum flows, which are critical components in dam design [1–3].

Some of the most commonly used theoretical probability distributions in the FFA are those from the Gamma family (Pearson III, Kritsky-Menkel, Log-Pearson), those from the generalized Pareto family (Pareto type II, III and IV, Wakeby) and those from the generalized extreme value family (Weibull, Frechet, Gumbel) [4–11]. Other distribution families, such as the beta generalized, beta prime, and beta exponential families, were recently added based on [12,13].

In terms of parameter estimation, in recent years, the use of these distributions in the FFA has focused on the L-moments [14,15], which is a much more stable parameter estimation method and less subject to bias [5–8,14–17], compared to other parameter estimation methods, namely the method of ordinary moments (MOM) or the maximum likelihood method (MLE), particularly for small and medium lengths of observed data. With all of these advantages over previous parameter estimate approaches, Anghel and Ilinca [18] discovered that the L-moments require some statistical indicator corrections. The least squares approach [18] can be used to rectify them. A good observation was also made by Gaume [17], who stated that the L-moments statistical indicators may be less affected by the series length variability, but this advantage can be lost due to nonlinear functions of parameter estimation.

Considering that in FFA, the area of interest is that of small annual exceeding probabilities (left-hand, rare events), it is necessary to fulfill the "separation effect" described by Matas [9], namely the elimination of the weight of small values (right-hand, lower part of the graph), since these do not always represent ''floods". This "separation effect" can be achieved using the higher order linear moments (LH-moments) approach. Wang proposed this method in 1997 [16], and it quickly became one of the most popular in the FFA, even without explicit sample censorship [14,16]. It is only approved for use in FFA with the Annual Maximum Series (AMS) [16]. This method is a generalization of the linear moments method [16], and it reduces the influence of small maximum values in frequency analysis. As a result, higher significance is given to high maximum values, which always represent floods. This method is usually used for low-flow frequency analysis [19], for flood frequency analysis [16,20–22], for regional flood frequency analysis [23–26] and for maximum rainfall frequency analysis [27–29].

In recent materials [30], important contributions have been made regarding the LH-moments, being presented important information for seven statistical distributions from the Gamma, Pareto, and GEV families.

In this article, we analyze the application of these two parameter estimation methods and we have formulated the L- and the LH-moments for all of the analyzed distribution (i.e., the PE3, the GEV, the W3, LL3, the LN3, the RY and the PG). The PE3 is also the main distribution in the FFA, in Romania [2–4,31–33]. Only these two parameter estimation methods are analyzed, since these are wanted to be included in the new normative in Romania. These methods present the main advantage of using the resulting statistical indicators for the regionalization process. Otherwise, the L-moments is the main parameter estimation method used in the regionalization processes.

The major goal of this article is to derive all of the elements required to use these distributions in FFA, particularly for distributions that do not have a close form for the inverse function. This is significant since these distributions employing the LH-moments approach are not yet included in dedicated applications.

This analysis represents also an extension, a development and a continuation of the research within the Faculty of Hydrotechnics, the results of which were presented in previous materials [3,12,13,18].

The following novelty elements, presented centrally in Table 1, are introduced for the first time in the scientific community. These will facilitate the application of these distributions in FFA, using the LH-moments method. These elements may also be applicable in other fields that require the performance of such statistical analyses.

Table 1. New elements presented in the manuscript.

Novelty	**Distribution**	
	Method	
	L-Moment	**LH-Moments**
Exact parameter estimation	Raylegh	Pearson III, Weibull, log-normal, generalized Pareto, Raylegh, log-logistic
Approximate estimation of parameters	GEV, Weibull, generalized Pareto, log-logistic	Pearson III, GEV, Weibull, log-normal, generalized Pareto, Raylegh, log-logistic
Expression of the quantile with the frequency factor (FF)	GEV, Weibull, Raylegh, log-normal	Pearson III, GEV, Weibull, log-normal, generalized Pareto, Raylegh, log-logistic

Table 1. *Cont.*

Novelty	**Distribution**	
	Method	
	L-Moment	**LH-Moments**
Exact relationships of the FF	GEV, Weibull, Raylegh, log-normal	Pearson III, GEV, Weibull, log-normal, generalized Pareto, Raylegh, log-logistic
Approximate estimation of the FF	GEV, Weibull, log-normal	Pearson III, GEV, Weibull, log-normal, generalized Pareto, Raylegh, log-logistic
The confidence interval with the Chow approach [34]	GEV, Weibull, generalized Pareto, log-normal, Raylegh, log-logistic	Pearson III, GEV, Weibull, log-normal, generalized Pareto, Raylegh, log-logistic
The skewness-kurtosis variation graph and relationships	Raylegh	Pearson III, GEV, Weibull, log-normal, generalized Pareto, Raylegh, log-logistic

Regarding the quantile function, Anghel and Ilinca provided for the first time, the inverse function using the FF for the L-moments [12,13,18]. The same methodology is applied to the LH-moments in this manuscript. Also, for the LH-moments, the confidence interval (C.I.) is expressed using Chow's relation for the first time, which uses the FF (see Table S1 from Supplementary File). Other important new data entered are the LH-skewness (τ_{H3})–LH-kurtosis (τ_{H4}) variation diagram (see Supplementary File).

For a faster calculation, but characterized by small errors, the estimation relations of these FF are presented (see Supplementary File).

Taking into account that, in some cases, it is necessary to solve non-linear systems of equations, for easy application approximation relations are presented. The relative errors of estimation are between 10^{-2} and 10^{-4}.

A FFA is performed, using the annual observed data for the Prigor River, Romania. The best model is chosen based on the statistical indicator values and diagrams, thus respecting the performance criteria specific to the analyzed methods.

Next, the article discusses and describes the statistical distributions, the parameter estimation method and the influence of sample length variability, in Section 2. In Section 3, an At-site case study is carried out using these distributions for the Prigor River. Sections 4 and 5 present the findings, discussion, and conclusions.

2. Methods

The FFA represents a direct way of finding out the maximum flows with small exceeding probabilities, using the annual observed data. The series consists of the maximum values that characterize each year, with the important mention that, in general, the lower maximum values of the series do not always represent floods. It is thus necessary to reduce the importance of these small maximum values, by fulfilling the so-called "separation effect". This can be achieved using the higher order linear moments method (LH-moments).

The stages in the development of FFA are according to international recommendations, summarized in Figure 1.

During the data curation step, the presence of outliers, homogeneity, and flow independence were verified. The observed data are homogeneous, independent, and no outliers were identified.

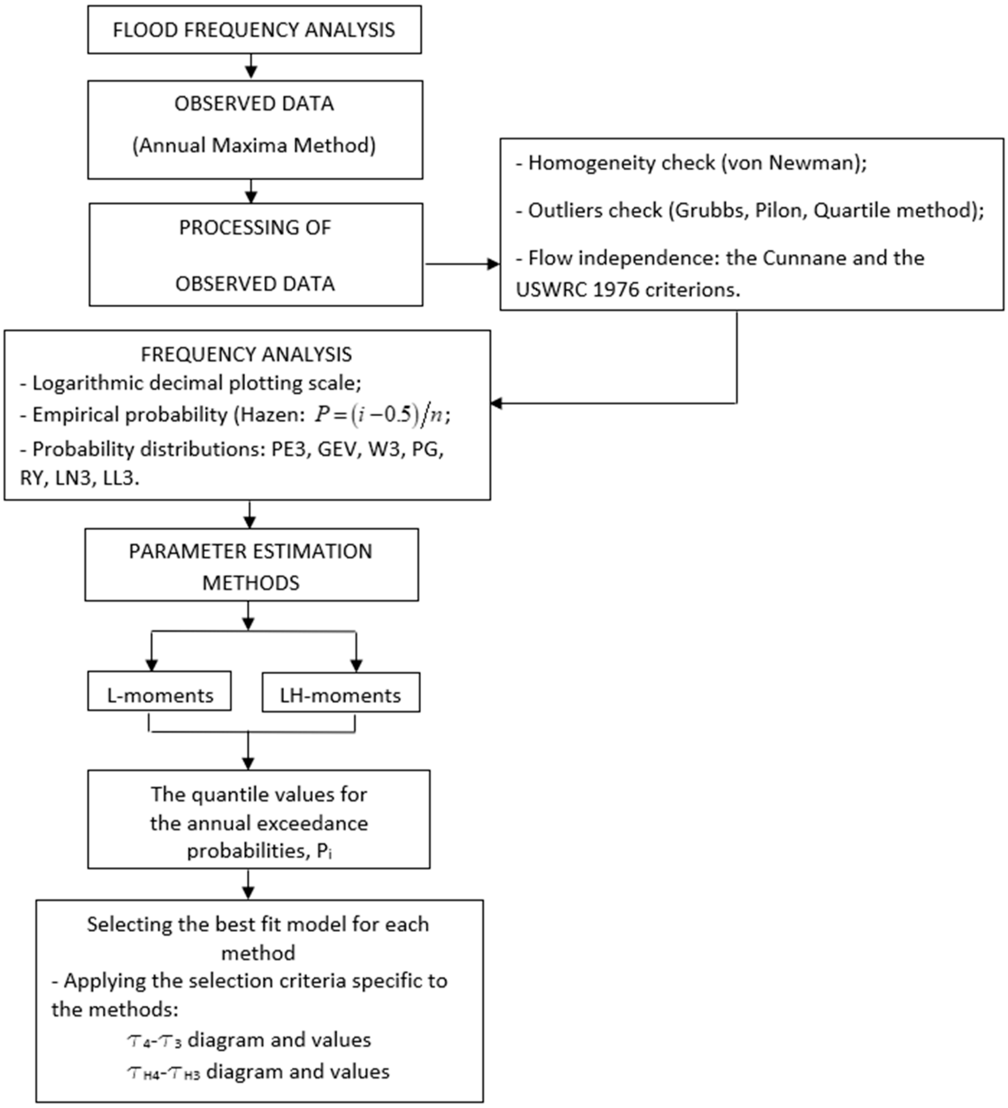

Figure 1. Methodological approach.

2.1. *Probability Distributions*

Table 2 shows the analyzed probability distributions [3–7,10,35–38]. It can be observed that the PE3 and LN3 distributions do not have close form for the quantile functions, they are represented in this manuscript using predefined functions from Mathcad, but which are equivalent in other dedicated programs such as Excel, etc. The predefined functions are detailed in [3].

Table 2. Distributions.

Distr.	Density Function $f(x)$	Complementary Cumulative Distribution Function $F(x)$	Inverse Function $x(p)$
PE3	$\frac{(x-\gamma)^{\alpha-1}}{\beta^{\alpha}\cdot\Gamma(\alpha)}\cdot\exp\left(-\frac{x-\gamma}{\beta}\right)$	$1-\frac{1}{\beta\cdot\Gamma(\alpha)}\cdot\int_{\gamma}^{x}\left(\frac{x-\gamma}{\beta}\right)^{\alpha-1}\cdot e^{-\frac{x-\gamma}{\beta}}dx$ $\frac{\Gamma\left(\alpha,\frac{x-\gamma}{\beta}\right)}{\Gamma(\alpha)}$	$\gamma+\beta\cdot qgamma(1-p,\alpha)$

Table 2. *Cont.*

Distr.	Density Function $f(x)$	Complementary Cumulative Distribution Function $F(x)$	Inverse Function $x(p)$
GEV	$\left(1-\frac{\alpha}{\beta}\cdot(x-\gamma)\right)^{\frac{1}{\alpha}-1}\cdot\frac{1}{\beta}\cdot e^{-\left(1-\frac{\alpha}{\beta}\cdot(x-\gamma)\right)^{\frac{1}{\alpha}}}$	$1-\exp\left(-\left(1-\frac{\alpha}{\beta}\cdot(x-\gamma)\right)^{\frac{1}{\alpha}}\right)$	$\gamma+\frac{\beta}{\alpha}\cdot\left(1-(-\ln(1-p))^{\alpha}\right)$
W3	$\frac{\alpha}{\beta}\cdot\left(\frac{x-\gamma}{\beta}\right)^{\alpha-1}\cdot e^{-\left(\frac{x-\gamma}{\beta}\right)^{\alpha}}$	$\exp\left(-\left(\frac{x-\gamma}{\beta}\right)^{\alpha}\right)$	$\gamma+\beta\cdot(-\ln(p))^{1/\alpha}$
GP	$\frac{1}{\beta}\cdot\left(1-\frac{\alpha}{\beta}\cdot(x-\gamma)\right)^{\frac{1}{\alpha}-1}$	$\left(1-\frac{\alpha}{\beta}\cdot(x-\gamma)\right)^{\frac{1}{\alpha}}$	$\gamma+\frac{\beta}{\alpha}\cdot(1-p^{\alpha})$
RY	$\frac{\left(\sqrt{\alpha^2+4\cdot\beta\cdot(x-\gamma)}-\alpha\right)\cdot e^{\frac{\alpha\cdot\sqrt{\alpha^2+4\cdot\beta\cdot(x-\gamma)}-\alpha^2-2\cdot\beta\cdot(x-\gamma)}{4\cdot\beta^2}}}{4\cdot\beta\cdot\sqrt{\alpha^2+4\cdot\beta\cdot(x-\gamma)}}$	$\exp\left(\frac{\sqrt{\alpha^2+4\cdot\beta\cdot(x-\gamma)}-\alpha}{2\cdot\beta\cdot\sqrt{2}}\right)^2$	$\gamma+\alpha\cdot\sqrt{\ln\left(\frac{1}{p^2}\right)}+\beta\cdot\ln\left(\frac{1}{p^2}\right)$ $\gamma+\alpha\cdot\sqrt{-2\cdot\ln(p)}-2\cdot\beta\cdot\ln(p)$
LN3	$\frac{\exp\left(-\frac{(\ln(x-\gamma)-\alpha)^2}{2\cdot\beta^2}\right)}{(x-\gamma)\cdot\beta\cdot\sqrt{2\cdot\pi}}$ $\frac{1}{x-\gamma}\cdot dnorm(\ln(x-\gamma),\alpha,\beta)$ $dlnorm(x-\gamma,\alpha,\beta)$	$1-\frac{1}{2}\cdot\left(erf\left(\frac{(\ln(x-\gamma)-\alpha)}{\sqrt{2}\cdot\beta}\right)+1\right)$ $1-pnorm(\ln(x-\gamma),\alpha,\beta)$ $1-cnorm\left(\frac{\ln(x-\gamma)-\alpha}{\beta}\right)$ $1-plnorm(x-\gamma,\alpha,\beta)$	$\gamma+e^{\alpha+\beta\cdot qnorm(1-p,0,1)}$ $\gamma+qlnorm(1-p,\alpha,\beta)$
LL3	$\frac{\alpha\cdot\left(\frac{x-\gamma}{\beta}\right)^{\alpha-1}\cdot\left(\left(\frac{x-\gamma}{\beta}\right)^{\alpha}+1\right)^{-2}}{\beta}$	$\left(1+\left(\frac{x-\gamma}{\beta}\right)^{\alpha}\right)^{-1}$	$\gamma+\beta\cdot\left(\frac{1}{p}-1\right)^{\frac{1}{\alpha}}$

2.2. Parameter Estimation Methods

In this manuscript, two methods of estimating the parameters of the proposed distributions are analyzed, namely the L- and the LH-moments. The L-moments method relies on linear combinations of weighted moments, whereas the LH-moments method is a generalization of the linear moments method that relies on linear combinations of higher-order statistics. This decreases the impact of lower maximum values, which do not always represent floods. As a result, the high maximum values—which invariably imply floods—are given more weight. For a better understanding and differentiation of the two methods, Supplementary File presents the characteristic theoretical relations of the methods.

All of the equations for estimating the parameters were determined based on the inverse function (see Appendix A), all equations representing new elements.

Given that in many cases, systems of nonlinear equations need to be solved, approximate relations for parameter estimation are presented (see Supplementary File).

Considering that the τ_3 and τ_{H3} indicators are, in general, characterized by a single parameter (the shape parameter), the presentation of the variation graphs helps to choose the initial values in the iterative process, simplifying the determination of the parameters of the distributions using the exact relations. Figure 2 shows the curves of the possible values of the shape parameter for the W3, PG, GEV, LL3, PE3, and LN3 distributions.

Regarding the approximate relationships for parameter estimation, the relative errors are between 10^{-2} and 10^{-4}. The errors depend only on the values of the L-skewness (τ_3) and LH-skewness (τ_{H3}) as can be seen in Figure 3. For the L-moments, the graphs were presented in previous materials [39].

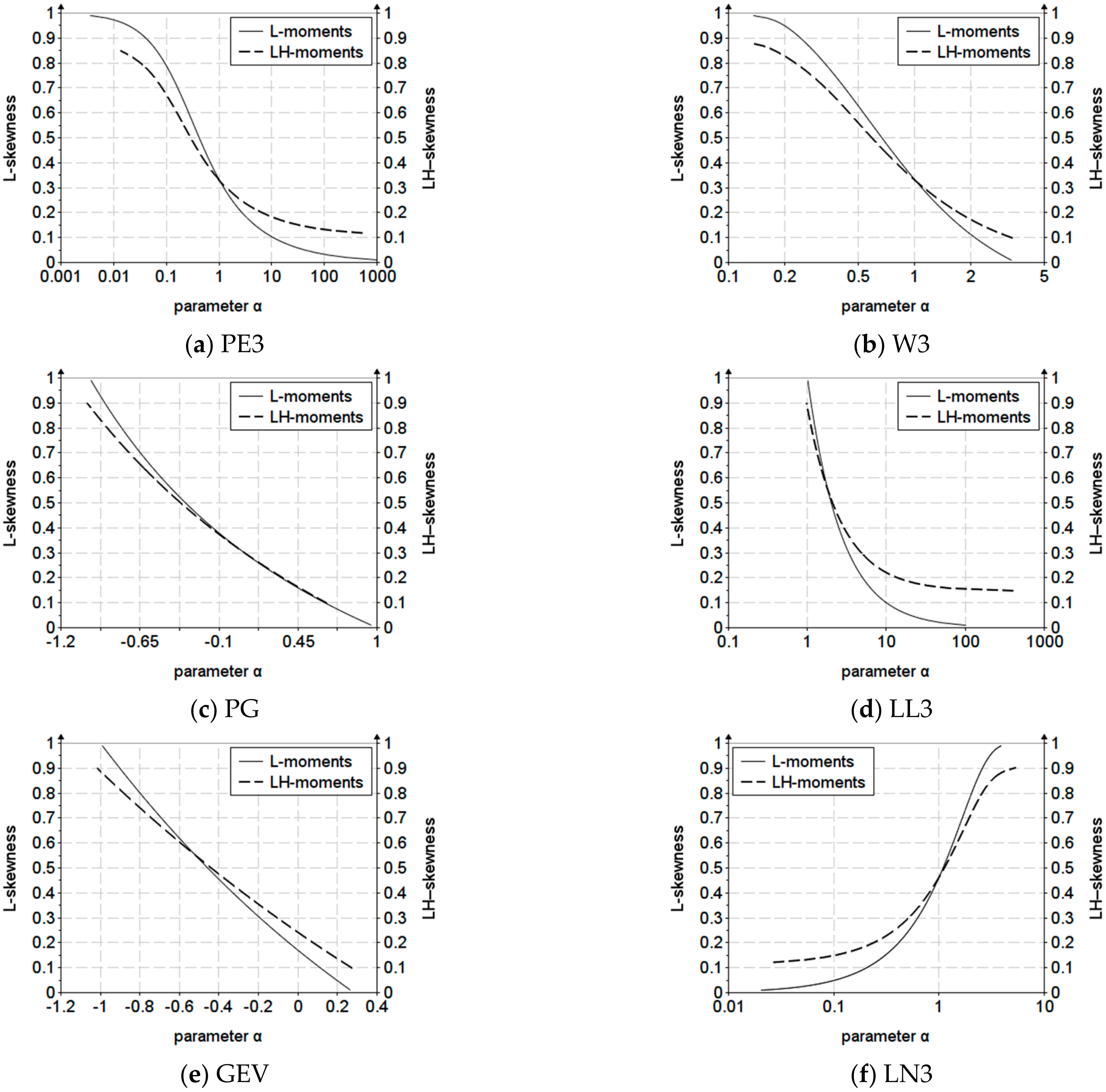

Figure 2. The curves of the possible values of the shape parameter, for the two analyzed methods.

Considering that the inverse function of each distribution can be represented using the FF characteristic of the method and the distribution, it is for the first time that, for these distributions, the exact and the approximate relationships for the FF are presented, using the L-moments and LH-moments method (see Supplementary File). This represents a real help in the easy and fast application of these distributions and methods in flood frequency analysis, thus being able to determine in an accessible way the values of the quantiles for the most common annual exceedance probabilities. The approximations of the FF do not depend on certain values of maximum annual flows, but they are determined based on the theoretical values of the high-order statistical indicators, thus leading to a reduction of the calculation time.

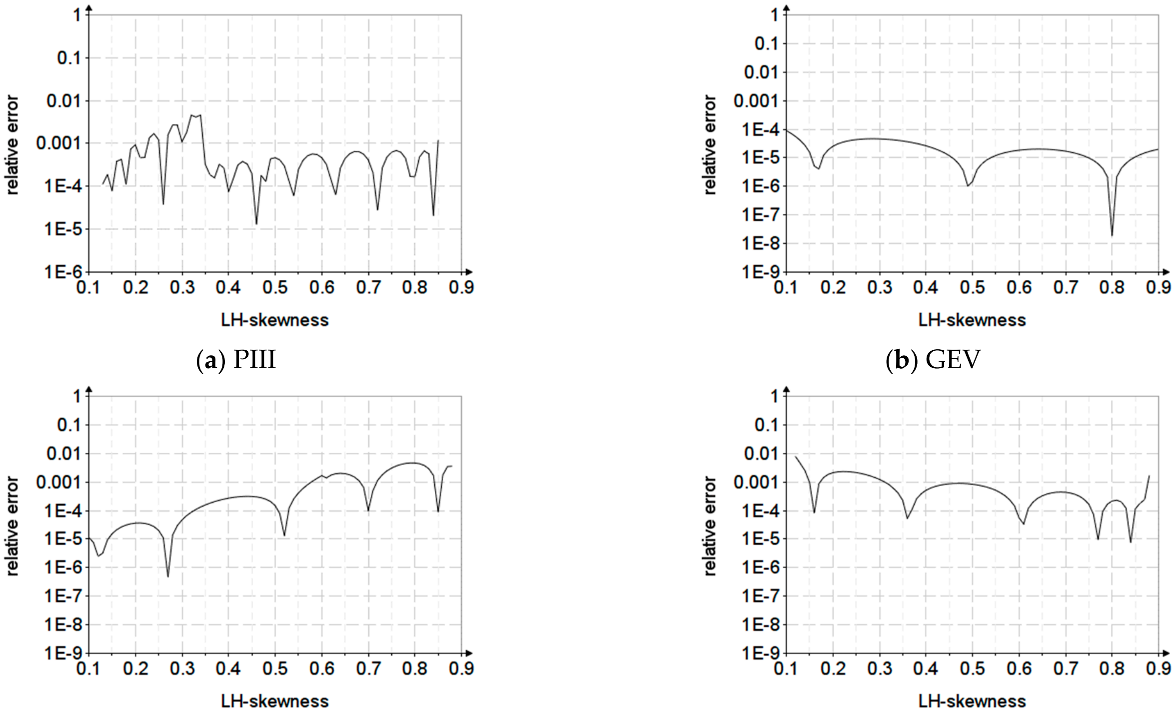

(**a**) PIII (**b**) GEV (**c**) W3 (**d**) LN3

Figure 3. The relative errors of estimating the parameters.

2.3. The Bias Due to the Length Variability of the Records

In general, for low annual exceedance probabilities, all three-parameter distributions have a large degree of uncertainty since they cannot calibrate the higher moments (L-kurtosis). Another significant issue is the uncertainty regarding the variability of the length of the data series, with each method characterized by uncertainties regarding the values of the statistical indicators, the values of the estimated parameters, and the values of the quantiles. However, when utilizing the L-moments technique, these three degrees of uncertainty are considerably decreased since it is less biased and more robust to sample variability.

The bias represents the deviation of the values obtained from the theoretical values specific to the distribution (characteristic for a population, n > 1000 values). This bias is influenced by the length of the data strings. It represents the difference between the theoretical value (population) and the calculated one (sample) in percentage.

A negative value of the bias means that the calculated values are higher than the theoretical values by that percentage (the obtained value should be corrected minus by that percentage). A positive value means that the calculated values are lower than the theoretical values, and should be increased by that percentage.

Thus, considering the relatively short length of the series analyzed in the case study (31 observed data), to highlight the statistical uncertainties characteristic of the three levels, the PG distribution is presented as example.

Assuming that the observed data are drawn from a PG distribution, starting from the theoretical values (specific to n $\approx$ 1000 values), by sampling (using the Hazen empirical formula), the new values of the statistical indicators, parameters and quantiles, as well as the bias compared to the theoretical values, are determined. For ease of calculations, the arithmetic mean is chosen.

2.3.1. The Bias for Statistical Indicators

Table 3 present the values of the theoretical statistical indicators and those obtained from sampling, for $\tau_3 = 0.3$ and $\tau_3 = 0.5$. These two values were chosen so as to reflect two distinct situations regarding the usual torrentiality and skewness encountered on rivers. The value 0.3 indicates a low skewness, while the value 0.5 indicates an average skewness. In both cases, the L-coefficient of variation (τ_2) is chosen 0.3.

Table 3. The bias for statistical indicators for PG and L-moments method.

PG							
	τ_3 = 0.3				**Bias [%]**		
Statistical Indicators	**Length (n)**				**Length (n)**		
	1000	**80**	**50**	**25**	**80**	**50**	**25**
L_1	1	0.998	0.997	0.994	0.2	0.3	0.6
τ_2	0.3	0.303	0.304	0.308	−1	−1.33	−0.8
τ_3	0.3	0.303	0.305	0.309	−1.09	−1.64	−2.91
τ_4	0.142	0.145	0.147	0.151	−2.11	−3.52	−6.34
$\tau_3 = 0.5$							
L_1	1	0.986	0.981	0.97	1.4	1.9	3
τ_2	0.3	0.294	0.292	0.29	2	2.67	3.33
τ_3	0.5	0.488	0.485	0.482	2.4	2.91	3.69
τ_4	0.318	0.304	0.301	0.297	4.4	5.35	6.6

In general, a holistic approach involves the highlighting of biases on the entire matrix defining the coefficient of L-variation indicators ($0 < \tau_2 < 1$), respectively L-skewness ($2 \cdot \tau_2 - 1 \leq \tau_3 < 1$). This aspect constitutes a future research direction, involving the Bootstrap, the Bayesian method and Monte Carlo simulations.

It can be seen from the resulting values that for low values of L-skewness the PG distribution has small bias. For the situation of higher values of L-skewness, the PG distribution is more affected being a distribution known as a heavy tail.

2.3.2. The Bias of Parameter Estimation

Regarding parameter estimate uncertainties, Gaume [17] stated that statistical indicators obtained with L-moments may be less affected by series length variation, but this advantage may be lost due to nonlinear functions of parameter estimation. Thus, in Table 4 the values of the parameters obtained from sampling are provided (as well as the bias compared to the theoretical values).

Table 4. The bias of parameter estimation for PG and L-moments.

PG							
	τ_3 = 0.3				**Bias [%]**		
Parameters	**Length (n)**				**Length (n)**		
	1000	**80**	**50**	**25**	**80**	**50**	**25**
α	0.077	0.069	0.065	0.056	10.39	15.58	27.27
β	0.671	0.688	0.667	0.664	0.45	0.6	1.04
γ	0.377	0.373	0.371	0.365	1	−1.62	3.18
$\tau_3 = 0.5$							
α	−0.333	−0.312	−0.307	−0.3	6.31	7.81	9.91
β	0.333	0.337	0.337	0.335	−1.2	−1.2	−0.6
γ	0.5	0.497	0.496	0.492	1	−0.81	1.6

2.3.3. The Bias of Quantiles Estimation

Considering that in the analysis of the frequency of extreme events it is desired to accurately determine the values of the maximum extreme events (rare events), the presentation of the bias due to the variability of the data series becomes of particular importance. Table 5 present the values of the quantiles obtained by sampling, as well as highlighting the relative errors compared to the theoretical values specific to the analyzed distributions, using the L-moments method.

Table 5. The bias of quantiles for PG and L-moments.

	PG						
	τ_3 = 0.3				Bias [%]		
Annual Exceedance Probability [%]	Length (n)				Length (n)		
	1000	80	50	25	80	50	25
0.01	4.81	4.92	4.99	5.14	−2.48	−3.75	−6.89
0.1	3.97	4.04	4.08	4.17	−1.74	−2.64	−4.83
0.5	3.30	3.34	3.36	3.41	−1.21	−1.82	−3.34
1	2.98	3.01	3.02	3.06	−0.97	−1.48	−2.69
	$\tau_3 = 0.5$						
0.01	21	18.5	18.0	17.1	12.07	14.69	18.91
0.1	9.5	8.7	8.5	8.2	8.14	10.04	13.26
0.5	5.3	5.1	5.0	4.8	5.52	6.92	9.41
1	4.1	4.0	3.9	3.8	4.44	5.65	7.82

As can be seen from the results, the L-moments is less affected by the variability of the length of the recorded data for small values of L-skewness ($\tau_3 < 0.5$), the bias of estimating the statistical indicators, and more important the quantiles (increasing with the increase of L-skewness).

For small values of available data (n = 25), the bias corresponding to the maximum flow with the probability of exceeding 0.01% can reach 18.91%, value much lower than those obtained using the MOM, values presented in previous materials [18] that reached over 40% compared to the theoretical value.

3. Case Study

The FFA aims to determine the maximum flows (particularly in areas of small annual excess probabilities) using the annual observed record for the Prigor River and the distributions presented, for the two parameter estimation approaches.

The Prigor River is located in the southwestern part of Romania, as seen in Figure 4 [40], and is the left tributary of the Nera River.

The region has a moderately temperate continental climate with sub-Mediterranean influences. This climate creates the mild nature of the temperature regime, the warmth intervals throughout the winter, and the multiannual average quantities of comparatively high precipitation between 550–1350 mm/year.

The multiannual average temperatures vary greatly over the territory, ranging from −3 °C in the mountains to 11 °C in the plains.

The river has a watershed area of 153 km^2 and a mean elevation of 713 m. The river is 33 km long and has a slope of 22‰. The sinuosity coefficient for the planned path of the river is 1.83 [41].

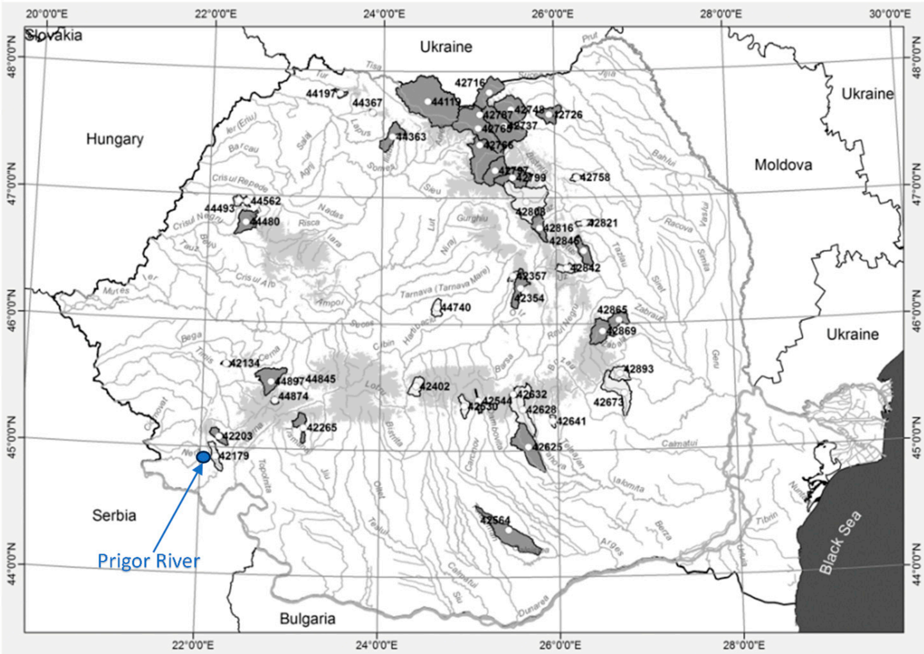

Figure 4. The Prigor River monitoring section.

The AMS over a 31-year period is used for FFA. The time period under consideration is 1990 through 2020. The top and lower values are 88 m^3/s and 6.4 m^3/s, respectively. Table 6 highlights the observed data values.

Table 6. The observed records for the Prigor River, Romania.

The AMS											
Year	**1990**	**1991**	**1992**	**1993**	**1994**	**1995**	**1996**	**1997**	**1998**	**1999**	**2000**
Flow [m^3/s]	9.96	15	10.1	14.8	7.30	21.2	18.2	21.4	13.1	14.5	35
	2001	**2002**	**2003**	**2004**	**2005**	**2006**	**2007**	**2008**	**2009**	**2010**	**2011**
Flow [m^3/s]	19.9	22.1	11.8	80.3	88	51.6	72.2	16.2	42.6	28.5	12.8
	2012	**2013**	**2014**	**2015**	**2016**	**2017**	**2018**	**2019**	**2020**		
Flow [m^3/s]	31.2	24.1	52.2	21.1	18.9	6.40	24.9	15.1	36.6		

The most important values in the analysis using the proposed methods are those of L-skewness, L-kurtosis, respectively LH-skewness and LH-kurtosis, since they are used to make an approximate estimation of the parameters of the analyzed distributions, as well as the regionalization of maximum flows.

For L-moments, the expected value (L_1), the L-coefficient of variation (τ_2), L-skewness (τ_3) and L-kurtosis (τ_4) are 27.2 m^3/s, 0.386, 0.399, respectively 0.228.

For first level LH-moments, the expected value (L_{H1}), the LH-coefficient of variation (τ_{H2}), LH-skewness (τ_{H3}) and LH-kurtosis (τ_{H4}) are 38.2 m^3/s, 0.292, 0.398, respectively 0.177.

4. Results and Discussion

The most essential quantiles in the FFA are those for low exceeding probability, since hydrotechnical structures, particularly dams, are planned using these quantiles [1,2].

As we stated before, only these two methods were analyzed in this article, since it represents two methods of estimating the parameters on the basis of which a regionalization can be carried out using the statistical indicators specific to the two methods.

Considering that currently in Romania the "parent" method is the MOM, in which the skewness is chosen according to the origin of the maximum flows [2,3], it is thus desirable to abandon this outdated practice and adopt the L- and LH-moments methods.

4.1. Parameter Estimation

The resulting values of the parameters are presented (see Table 7) for transparency of the analysis and the possibility that the results can be reproduced.

Table 7. The parameters values for the case study.

Parameters	**Distribution**						
	PE3	**GEV**	**W3**	**PG**	**RY**	**LN3**	**LL3**
				L-moments			
α	0.6937	−0.3277	0.848	−0.1402	−8.67	2.601	2.5083
β	26.9	10.2	17.6	17.1	13.9	0.9569	20.3
γ	8.97	16.9	8.51	7.78	10.8	6.34	0.854
				LH-moments			
α	0.5828	−0.2708	0.8057	−0.1496	−14.9	2.8904	2.9638
β	29.5	11.5	16.2	16.8	15.8	0.8078	27.2
γ	11.5	16.5	9.57	7.98	15.2	2.6013	−5.95

4.2. Quantile Estimation

Only the values of the quantiles for the usual and most important annual exceedance probabilities in FFA are presented (see Table 8), paying special attention to the values characteristic of very rare events that need to be forecast (left-hand, upper part of the graph).

Table 8. Quantile values for the case study.

Distr.	**Annual Exceedance Probabilities [%]**																	
	L-Moments									**LH-Moments**								
	0.01	**0.1**	**0.5**	**1**	**2**	**3**	**5**	**80**	**90**	**0.01**	**0.1**	**0.5**	**1**	**2**	**3**	**5**	**80**	**90**
PE3	231	172	130	113	95.4	85.3	72.7	11.4	9.80	239	176	133	114	96.3	85.8	72.8	13.1	12.0
GEV	623	285	163	127	97.7	83.6	68.2	12.4	9.50	489	250	152	122	96.3	83.5	69.0	11.4	7.90
W3	249	180	134	115	96.2	85.6	72.5	11.5	9.75	264	188	138	117	97.5	86.3	72.7	12.1	10.6
PG	329	207	142	118	96.8	85.1	71.4	11.7	9.59	340	211	143	119	97.0	85.2	71.3	11.8	9.76
RY	229	170	130	112	95.0	85.0	72.6	11.2	9.72	242	178	134	115	96.9	86.3	73.2	12.2	11.6
LN3	480	266	165	132	103	87.9	71.4	12.4	10.3	366	221	147	121	97.2	84.9	70.6	11.7	8.99
LL3	800	320	168	128	96.7	82.1	66.6	12.5	9.31	603	274	157	123	95.3	82.1	67.6	11.1	7.03

Figure 5 show the distributions curves for the Prigor River. For linear moments method, the best choice for plotting-position are Hazen and IEC 56 empirical probability [42]. In this case study, the Hazen empirical probability was used ($P = (i - 0.5)/n$).

The decimal logarithmic scale on the horizontal axis was used to highlight the heavy tail (the domain of low annual exceedance probabilities).

Analyzing the values obtained for the probability of exceeding 0.01% (return period of 1000 years) it can be seen that the PE3, W3, PG, and RY distributions are the least sensitive, since if we analyze the variation of the shape parameter, they practically intersect in around the value corresponding to the skewness of the records. For both methods, the results of the PE3, W3, PG, and RY distributions remain relatively constant around the value of 240 m^3/s (PE3, RY, W3), respectively 320 m^3/s (PG).

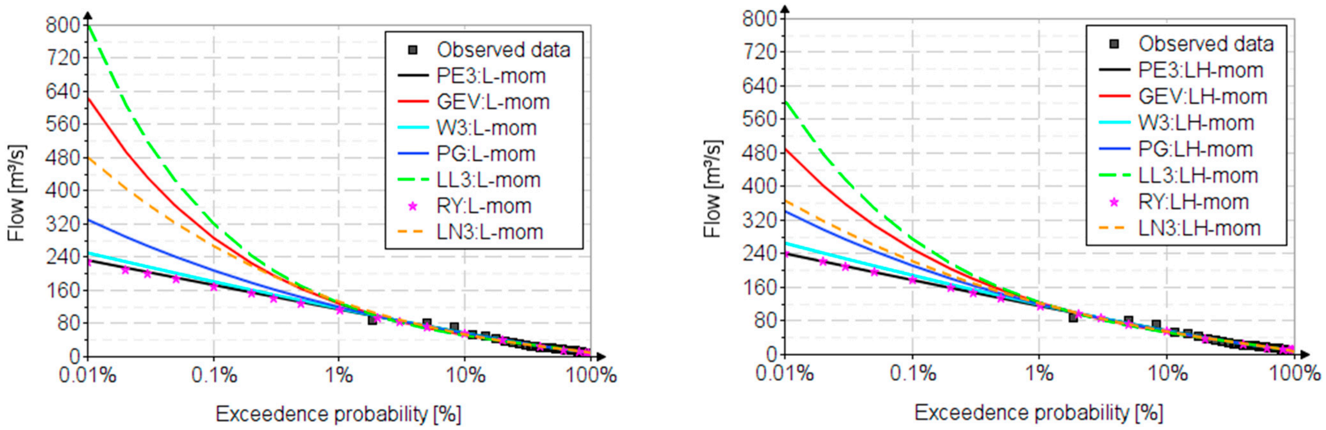

Figure 5. The graphic representation of the quantile function.

For the GEV, LL3 and LN3 distributions, the variation is large around this value, which is why a significant difference can be observed between the two methods. The results, between the two methods, vary between 623 m^3/s and 489 m^3/s for GEV distribution, between 480 m^3/s and 366 m^3/s for LN3 distribution, respectively between 800 m^3/s and 603 m^3/s for LL3 distribution. Comparing the results it can be seen that the LH-moments achieves to some extent the "separation effect", by reducing the importance of the maximum flows from the field of high annual exceedance probabilities (right-hand, lower part of the graph), which do not always constitute (in the analysis with AMS) floods.

4.3. Performance Metrics

The performance and choosing the best fitted model, was evaluated using the criteria specific to the analyzed methods, namely the linear and higher order linear moments values and diagrams.

In the case of L-moment analysis, the best model is characterized by the τ_3 and τ_4 values, so that the difference between the natural values of the theoretical distribution and the values of the observed data to be minimal [3,5,15,18]. The same principle is used in the analysis with the LH-moments method.

Evidence of these selection criteria is critical, particularly for the FFA in Romania, where the current laws [43] are severely deficient. It suggests using a variety of two and three parameter distributions with various parameter estimation methods, keeping in mind that the results obtained with a two-parameter distribution using the MOM cannot be compared to the results obtained with a three-parameter distribution using L-moments, or vice versa. The regulation suggests that you select any distribution that falls between the lower distribution (a distribution that can be a two parameters and the L-moments technique) and the upper distribution (a distribution than can be a three parameters and the MOM technique).

Table 9 shows the analyzed distributions performance measures values. The performance measures for the best distribution are marked in bold.

The RME and RAE criterion can only be used in the probability area of the records (area of empirical probabilities), the data set being too short, for these indicators to highlight certain performances of the distributions, over the entire range of annual exceedance probabilities.

Based on [3,13,18,37], the diagram for the L-moments contains a significant number of theoretical distributions usually used in hydrology.

Regarding the diagram for the LH-moments, it is for the first time that such a diagram is presented and introduced to the scientific community, as well as the explicit variation relationships of the $\tau_{H3} - \tau_{H4}$ (see Supplementary File).

Table 9. Distributions performance measures for the Prigor River, Romania.

Distr.	Performance Measures											
	Methods for Parameter Estimation								Selection Criteria			
	L-Moments				LH-Moments				L-Moments		LH-Moments	
	RME	RAE	τ_3	τ_4	RME	RAE	τ_{H3}	τ_{H4}	τ_3	τ_4	τ_{H3}	τ_{H4}
PE3	0.0219	0.0885		0.192	0.0301	0.0953		0.197				
GEV	0.0152	0.0636		0.282	0.0213	0.0925		0.250				
W3	0.0201	0.0822		0.202	0.0245	0.0850		0.206				
PG	0.0181	0.0765	**0.399**	**0.221**	0.0187	0.0766	**0.398**	0.221	0.399	0.228	0.398	0.177
RY	0.0237	0.0955		0.185	0.0391	0.1133		**0.192**				
LN3	0.0199	0.0759		0.280	0.0148	0.0673		0.233				
LL3	0.0165	0.0715		0.299	0.0307	0.1204		0.265				

Figure 6 shows the variation diagrams of the $\tau_3 - \tau_4$ obtained with the two methods, highlighting the values of the data.

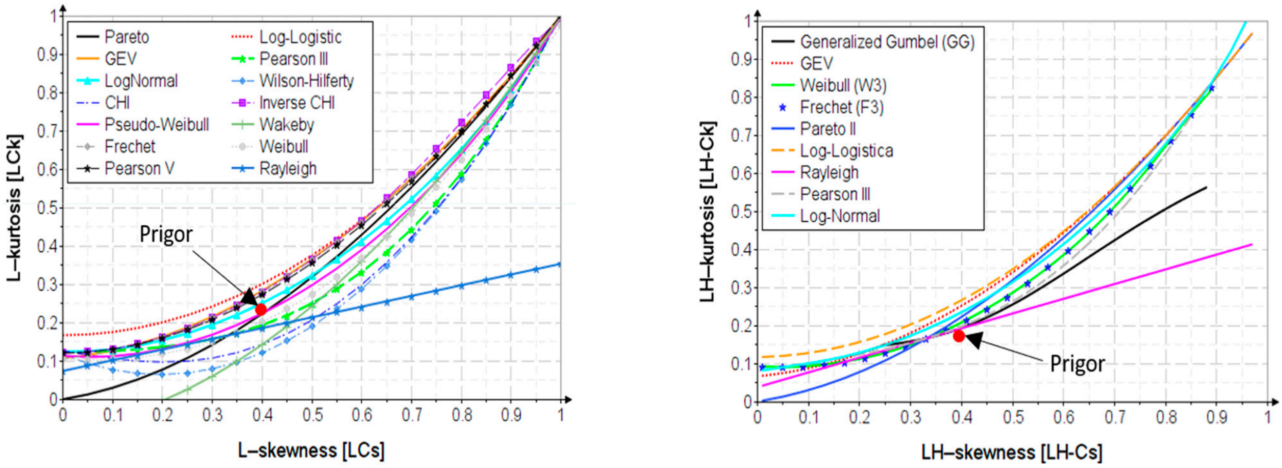

(**a**) L-moments (**b**) LH-moments

Figure 6. The variation diagram of skewness and kurtosis.

Thus, according to these performance criteria (imposed by the analyzed methods), based on the results and confirmed also by the graphic representation, the best fitted model for the L-moments is the PG distribution with $\tau_3 = 0.399$ and $\tau_4 = 0.221$, respectively the RY distribution for the LH-moments method with $\tau_{H3} = 0.398$ and $\tau_{H4} = 0.192$. The indicator values of these two distributions are closest to those of the data recorded, namely $\tau_3 = 0.399$, $\tau_4 = 0.228$, $\tau_{H3} = 0.398$ and $\tau_{H4} = 0.177$.

The resulting maximum flow values (for the annual probability of exceeding 0.01%) are 329 m^3/s (L-moments) and 239 m^3/s (LH-moments) in the case of PG distribution, respectively 229 m^3/s and 242 m^3/s in the case of RY distribution.

Analyzing the results of these distributions with those of other distributions used on the same case study (Pseudo-Weibull and three-parameter Chi distribution) it can be seen that the values are similar [30].

4.4. The Bias Due to the Length Variability of the Records

To exemplify the influence of the variability of the analyzed data lengths on the results obtained, the bias in the estimation of the quantile values corresponding to the annual exceedance probabilities of 0.01%, 0.1%, 0.5% and 1% is highlighted (for the L-moments).

Given that the PG distribution was found to be the best model for the L-moments, it is reasonable to conclude that the observed data is derived from a PG distribution. Thus, the bias of the quantiles for the length of the investigated series (n = 31) are those shown in Table 10 for the L-moments approach.

Table 10. The bias of quantiles for the Prigor River.

τ_2 = 0.386, τ_3 = 0.399 **n = 31**	**Annual Exceedance Probability [%]**			
P%	**0.01**	**0.1**	**0.5**	**1**
Bias [%]	1.3	1.19	1.13	1.1

It can be observed that for the analyzed case study, the biases that characterize the L-moments, with values between 1.3% for the quantile with a return period of 10,000 years, respectively 1.1% for the event with a return period of 100 years, are very small, the statistical errors being more than acceptable.

4.5. Confidence Intervals

Given all of these statistical uncertainties caused by the variability of data lengths, the confidence interval (C.I.) of the inverse function must be presented (see Figure 7).

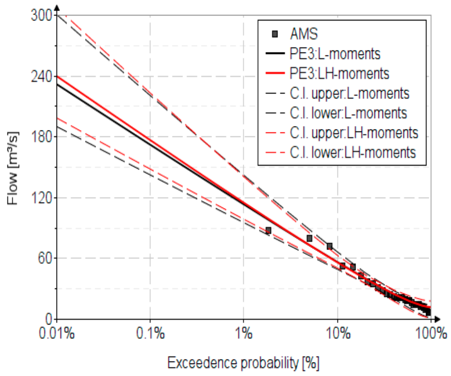

(**a**) PE3

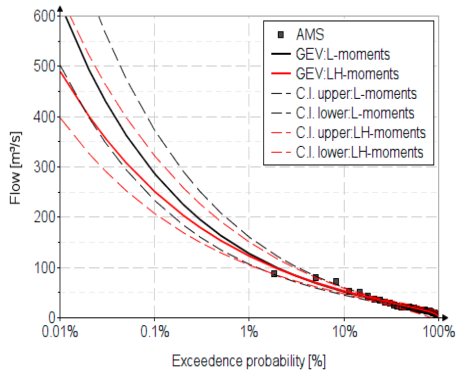

(**b**) GEV

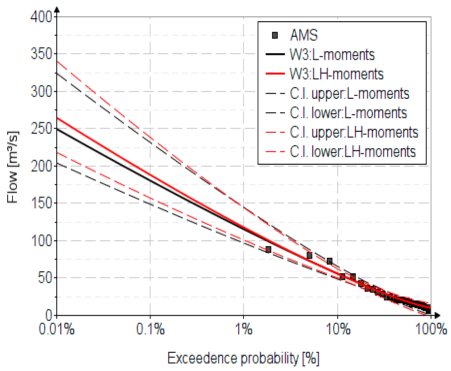

(**c**) W3

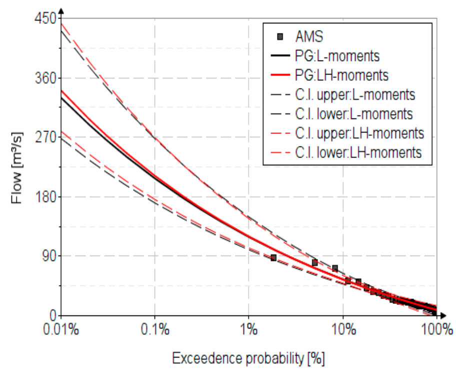

(**d**) PG

Figure 7. *Cont.*

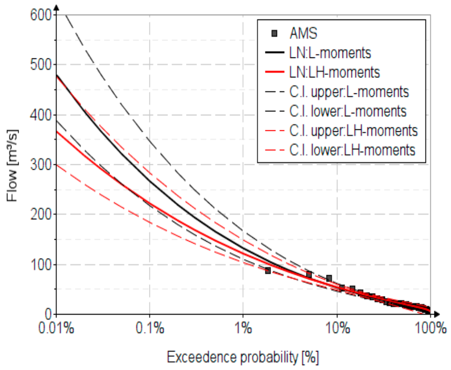

(**e**) LN3

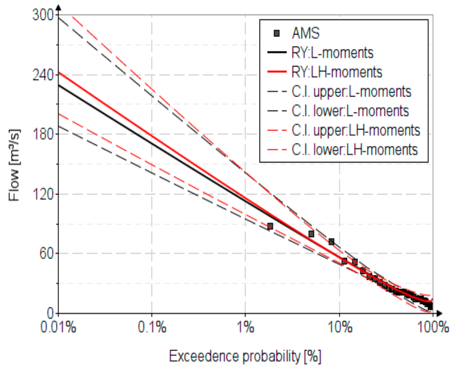

(**f**) RY

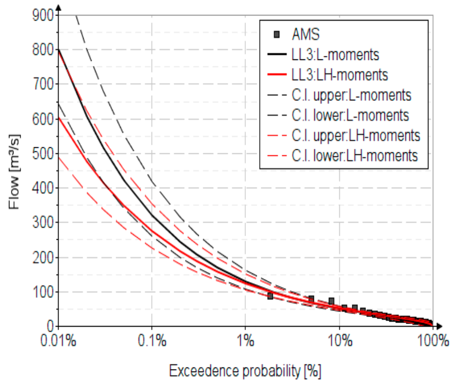

(**g**) LL3

Figure 7. Curves of probability distributions with confidence intervals.

The C.I. is based on the FF of the distribution, using Chow's relation, for a 95% confidence level and a Gaussian assumption. The classic Bootstrap procedure [44–48] is another way for estimating the confidence interval, although it is more time consuming and has certain drawbacks.

5. Conclusions

This manuscript analyzes the L-moments and LH-moments, which are two of the most commonly employed methods in FFA, since they are less influenced by sample variability and the presence of outliers.

The main purpose of this manuscript is to provide all of the essentials for applying a variety of seven theoretical probability distributions using these methods for parameter estimation. In general, the entire analysis focuses only on the statistical aspects related to FFA. The analysis does not exclude the use of other statistical distributions or methods.

Thus, exact and approximate relations to derive the parameters and the FF are presented for the first time. In addition, relationships and their variation diagrams are presented for the LH-moments method, being of signficant help in applying these distributions using this method. The choice of the best suitable distribution, in the case of both methods, is carried out by reporting the values of the statistical indicators (L-skewness and L-kurtosis, and LH-skewness and LH-kurtosis) to the values of the observed data. Regarding the L-moments method, based on the work of Anghel and Ilinca [18,39,49], the variation diagram for the L-moments was much improved with a significantly higher number of distributions compared to the previously existing situation in the literature [5,6].

All of these new elements were used to determine the maximum flows for the chosen annual exceedance probabilities, using the Prigor river in Romania as a case study. Following the results obtained (only from the analyzed distributions), the best model are the PG distribution for the L-moments, respectively the RY distribution for the LH-moments.

Their natural indicators (L-skewness, L-kurtosis, LH-skewness, and LH-kurtosis), have the closest values to those of the observed data.

Since the use of software without mathematical knowledge frequently leads to flawed analyses, mathematical support in statistical analysis is useful. All of the math needed to use these distributions is necessary since statistical analysis software is limited.

As with other types of distributions, all of these new elements can be useful to researchers, only if the main statistical criteria specific to these methods are respected.

All of the information will be concretized in informative applications that will be included in the future proposals regarding the development of norms regarding the frequency analysis of maximum flows, giving up the old Soviet influences and avoiding the use of no-technical concepts such as the uncertainty interval [50].

Supplementary Materials: The following supporting information can be downloaded at: https://www.mdpi.com/article/10.3390/w15193510/s1. Figure S1: The L−skewness and L−kurtosis variation; Figure S2: The variation diagram for LH−skewness and LH−kurtosis. Table S1: Frequency factors; Table S2: The frequency factor with LH−moments for Pearson III; Table S3: The frequency factor for Log−normal; Table S4: The frequency factor for estimation with LH−moments for Log−normal; Table S5: The frequency factor for estimation with LH−moments for Log−logistic; Table S6: The frequency factor for estimation with L−moments for generalized Pareto; Table S7: The frequency factor for generalized Pareto; Table S8: The frequency factor for GEV; Table S9: The frequency factor for estimation with LH−moments for GEV; Table S10: The frequency factor for Weibull; Table S11: The frequency factor for estimation with LH−moments for Weibull.

Author Contributions: Conceptualization, C.G.A., S.C.S. and C.I.; methodology, C.G.A., S.C.S. and C.I.; software, C.G.A., S.C.S. and C.I.; vali-dation, C.G.A., S.C.S. and C.I.; formal analysis, C.G.A., S.C.S. and C.I.; investigation, C.G.A., S.C.S. and C.I.; resources, C.G.A., S.C.S. and C.I.; data curation, C.G.A., S.C.S. and C.I.; writing—original draft preparation C.G.A. and C.I.; writing—review and editing, C.G.A., S.C.S. and C.I.; visualization, C.G.A., S.C.S. and C.I.; supervision, C.I. and C.G.A.; project administration, C.G.A., S.C.S. and C.I.; funding acquisition, C.G.A., S.C.S. and C.I. All authors have read and agreed to the published version of the manuscript.

Funding: This research received no external funding.

Data Availability Statement: Not applicable.

Conflicts of Interest: The authors declare no conflict of interest.

Abbreviations

MOM	The method of ordinary moments
L-moments	The method of linear moments
LH-moments	The method of higher order linear moments
LHC_s, τ_{H3}	LH-skewness
LHC_v, τ_{H2}	coefficient of LH variation
LHC_k, τ_{H4}	LH-kurtosis
μ	Expected value; arithmetic mean
σ	Standard deviation
σ^2	Variance
C_v	Coefficient of variation
C_s	Coefficient of skewness; skewness
C_k	Coefficient of kurtosis; kurtosis
L_1, L_2, L_3	Linear moments
τ_2, LC_v	Coefficient of variation based on the L-moments method
τ_3, LC_s	Coefficient of skewness based on the L-moments method
τ_4, LC_k	Coefficient of kurtosis based on the L-moments method
FFA	Flood frequency analysis
Distr.	Distributions
AMS	Annual maximum series
RME	Relative mean error

RAE	Relative absolute error
n	Observed values length
$\Gamma(\alpha)$	$\int_0^\infty t^{\alpha-1} \cdot e^{-t} \cdot dt$, returns the value of the Euler gamma function of α
$\Gamma(\alpha, x)$	$\int_x^\infty t^{\alpha-1} \cdot e^{-t} \cdot dt$, returns the value of the incomplete gamma function of x with parameter α
$qgamma(p, \alpha)$	Returns the inverse cumulative probability distribution for probability p, for gamma distribution
$plnorm(x, \alpha, \beta)$	Returns the cumulative probability distribution for value x, for log-normal distribution
$pnorm(x, \alpha, \beta)$	Returns the cumulative probability distribution for value x, for normal distribution
$qlnorm(p, \alpha, \beta)$	Returns the inverse cumulative probability distribution for probability p, for log-normal distribution
$cnorm(x)$	Returns the cumulative probability distribution with mean 0 and variance 1 (normal distribution)
$dnorm(x, \alpha, \beta)$	Returns the probability density for value x, for normal distribution
$dlnorm(x, \alpha, \beta)$	Returns the probability density for value x, for log-normal distribution

Appendix A. The First Order LH-Moments for PE3, GEV, W3, PG, LL3 and RY Distributions

Appendix A.1. Pearson III (PE3)

For the L-moment and LH-moments, the parameters are calculated using definite integrals and quantile functions.

For the L-moments, α can be approximate with the next relation [45]:
if $0 < |\tau_3| \le \frac{1}{3}$:

$$\alpha = \exp\left(\begin{array}{l} -3.164791927 - 5.108735285 \cdot \ln(|\tau_3|) - 4.116014079 \cdot \ln(|\tau_3|)^2 - \\ 2.985250105 \cdot \ln(|\tau_3|)^3 - 1.327399577 \cdot \ln(|\tau_3|)^4 - 0.373944875 \cdot \ln(|\tau_3|)^5 - \\ 0.065421611 \cdot \ln(|\tau_3|)^6 - 0.006508037 \cdot \ln(|\tau_3|)^7 - 0.000281969 \cdot \ln(|\tau_3|)^8 \end{array}\right)$$

if $\frac{1}{3} < |\tau_3| \le \frac{2}{3}$:

$$\alpha = \exp\left(\begin{array}{l} -3.9918551 - 10.781466 \cdot \ln(|\tau_3|) - 21.557807 \cdot \ln(|\tau_3|)^2 - \\ 33.8752604 \cdot \ln(|\tau_3|)^3 - 35.0641585 \cdot \ln(|\tau_3|)^4 - 22.921163 \cdot \ln(|\tau_3|)^5 - \\ 8.5491823 \cdot \ln(|\tau_3|)^6 - 1.3855653 \cdot \ln(|\tau_3|)^7 \end{array}\right)$$

if $\frac{2}{3} < |\tau_3| < 1$:

$$\alpha = \frac{\begin{array}{l} 5.17817436 - 26.209448756 \cdot |\tau_3| + 62.12494027 \cdot \tau_3^2 - 84.39423264 \cdot |\tau_3|^3 + \\ 67.08589624 \cdot \tau_3^4 - 29.150288079 \cdot |\tau_3|^5 + 5.364968945 \cdot \tau_3^6 \end{array}}{1 + 0.0005134 \cdot |\tau_3| + 0.00063644 \cdot \tau_3^2}$$

$$\beta = L_2 \cdot \sqrt{\pi} \cdot \frac{\Gamma(\alpha)}{\Gamma\left(\alpha + \frac{1}{2}\right)}$$

$$\gamma = L_1 - \alpha \cdot \beta$$

For the LH-moments method, α can be approximate with the next relation:
if $0.12 < |\tau_{H3}| \le 0.34$:

$$\alpha = \exp\left(\begin{array}{l} 7757.0921831 + 40914.6033757 \cdot \ln(|\tau_{H3}|) + 93713.9484593 \cdot \ln(|\tau_{H3}|)^2 + \\ 121792.0331514 \cdot \ln(|\tau_{H3}|)^3 + 98255.1222272 \cdot \ln(|\tau_{H3}|)^4 + 50397.8680523 \cdot \ln(|\tau_{H3}|)^5 + \\ 16054.8135102 \cdot \ln(|\tau_{H3}|)^6 + 2904.9945626 \cdot \ln(|\tau_{H3}|)^7 + 228.664592 \cdot \ln(|\tau_{H3}|)^8 \end{array}\right)$$

if $0.34 < |\tau_{H3}| \leq 0.85$:

$$\alpha = \exp\left(\begin{array}{l} -13.4247904 - 121.5293664 \cdot \ln(|\tau_{H3}|) - 649.9763722 \cdot \ln(|\tau_{H3}|)^2 - \\ 2075.3170378 \cdot \ln(|\tau_{H3}|)^3 - 4110.4652507 \cdot \ln(|\tau_{H3}|)^4 - 5114.9286399 \cdot \ln(|\tau_{H3}|)^5 - \\ 3890.8525714 \cdot \ln(|\tau_{H3}|)^6 - 1653.2523283 \cdot \ln(|\tau_{H3}|)^7 - 300.612615 \cdot \ln(|\tau_{H3}|)^8 \end{array}\right)$$

$$\beta = \frac{2 \cdot L_{H2}}{3 \cdot z_1}$$

$$\gamma = L_{H1} - 2 \cdot \beta \cdot z_2$$

where, $z_1 = \int_0^1 qgamma(p, \alpha) \cdot \left(3 \cdot p^2 - 2 \cdot p\right) \cdot dp$, which can be approximated with the following equation:

$$z_1 = \frac{-0.00315255 + 0.87292281 \cdot \alpha + 0.18314623 \cdot \alpha^2}{1 + 2.01526823 \cdot \alpha + 0.07089912 \cdot \alpha^2 - 0.00034641 \cdot \alpha^3 + 0.00000094 \cdot \alpha^4}$$

and, $z_2 = \int_0^1 qgamma(p, \alpha) \cdot p \cdot dp$, which can be approximated with the following equation:

$$z_2 = \frac{0.01180195 + 0.87724953 \cdot \alpha + 0.46798927 \cdot \alpha^2 + 0.01808637 \cdot \alpha^3 + 0.00004649 \cdot \alpha^4}{1 + 0.80457526 \cdot \alpha + 0.03470298 \cdot \alpha^2 + 0.0000921 \cdot \alpha^3}$$

Appendix A.2. Generalized Extreme Value (GEV)

For the L-moments method, the exact equations are [6]:

$$L_1 = \gamma + \frac{\beta}{\alpha} \cdot (1 - \Gamma(1 + \alpha))$$

$$L_2 = \Gamma(\alpha) \cdot \left(1 - 2^{-\alpha}\right) \cdot \beta$$

$$L_3 = \Gamma(\alpha) \cdot \left(1 - 2^{-\alpha}\right) \cdot \beta \cdot \left(\frac{\left(1 - 3^{-\alpha}\right) \cdot 2}{1 - 2^{-\alpha}} - 3\right)$$

Parameter α can be approximate using the next relation depending on τ_3:

$$\alpha = \frac{0.283759107 - 1.669931462 \cdot |\tau_3|}{1 + 0.441588375 \cdot |\tau_3| - 0.071007671 \cdot \tau_3^2 + 0.015634368 \cdot |\tau_3|^3}$$

$$\beta = \frac{L_2}{\Gamma(\alpha) \cdot (1 - 2^{-\alpha})}$$

$$\gamma = L_1 + \frac{\beta}{\alpha} \cdot (\Gamma(1 + \alpha) - 1)$$

For the LH-moments method, the exact equations are [20]:

$$L_{H1} = \gamma + \frac{\beta}{\alpha} \cdot \left(1 - \Gamma(1 + \alpha) \cdot 2^{-\alpha}\right)$$

$$L_{H2} = \frac{3}{2} \cdot \frac{\beta}{\alpha} \cdot \Gamma(1 + \alpha) \cdot \left(2^{-\alpha} - 3^{-\alpha}\right)$$

$$L_{H3} = \frac{2}{3} \cdot \frac{\beta}{\alpha} \cdot \Gamma(1 + \alpha) \cdot \left(8 \cdot 3^{-\alpha} - 5 \cdot 4^{-\alpha} - 3 \cdot 2^{-\alpha}\right)$$

Parameter α can be approximate using the next relation depending on τ_{H3}:

$$\alpha = \frac{0.481461312 - 2.091126798 \cdot |\tau_{H3}| + 0.46287569 \cdot \tau_{H3}{}^2}{1 + 0.10816836 \cdot |\tau_{H3}| - 0.118896764 \cdot \tau_{H3}{}^2 + 0.013328421 \cdot |\tau_{H3}|^3}$$

$$\beta = \frac{-2 \cdot L_{H2}}{\Gamma(\alpha) \cdot 3 \cdot (3^{-\alpha} - 2^{-\alpha})}$$

$$\gamma = L_{H1} - \frac{\beta}{\alpha} \cdot \left(1 - \Gamma(1+\alpha) \cdot 2^{-\alpha}\right)$$

Appendix A.3. Weibull (W3)

For the L-moments, the parameters for the W3 distribution are obtained using the following expressions [6,34]:

$$L_1 = \gamma + \beta \cdot \Gamma\left(1 + \frac{1}{\alpha}\right)$$

$$L_2 = \beta \cdot \Gamma\left(1 + \frac{1}{\alpha}\right) \cdot \left(1 - 2^{-\frac{1}{\alpha}}\right)$$

$$L_3 = \beta \cdot \Gamma\left(1 + \frac{1}{\alpha}\right) \cdot \left(1 - 2^{-\frac{1}{\alpha}}\right) \cdot \left(2 \cdot \frac{2^{-\frac{1}{\alpha}} - 3^{-\frac{1}{\alpha}}}{2^{-\frac{1}{\alpha}} - 1} + 1\right)$$

Parameter α has the following approximate forms depending on τ_3:

$$\alpha = \frac{3.528107902 - 6.294082546 \cdot |\tau_3| + 2.767652838 \cdot \tau_3^2}{1 + 4.599024923 \cdot |\tau_3| - 7.993601572 \cdot \tau_3^2 + 2.423742593 \cdot |\tau_3|^3}$$

$$\beta = \frac{L_2}{\Gamma\left(1 + \frac{1}{\alpha}\right) \cdot \left(1 - 2^{-\frac{1}{\alpha}}\right)}$$

$$\gamma = L_1 - \frac{\beta}{\alpha} \cdot \Gamma\left(\frac{1}{\alpha}\right)$$

For the LH-moments method, the exact equations are:

$$L_{H1} = \gamma - \frac{\beta}{\alpha} \cdot \left(\Gamma\left(\frac{1}{\alpha}\right) \cdot 2^{-\frac{1}{\alpha}} + 2 \cdot \Gamma\left(\frac{1}{\alpha}\right)\right)$$

$$L_{H2} = \frac{\beta}{2 \cdot \alpha} \cdot \Gamma\left(\frac{1}{\alpha}\right) \cdot \left(3^{1-\frac{1}{\alpha}} + 3 - 3 \cdot 2^{1-\frac{1}{\alpha}}\right)$$

$$L_{H3} = \frac{2 \cdot \beta}{3 \cdot \alpha} \cdot \Gamma\left(\frac{1}{\alpha}\right) \cdot \left(4 \cdot 3^{1-\frac{1}{\alpha}} + 2 - 5 \cdot 2^{-\frac{2}{\alpha}} - 9 \cdot 2^{-\frac{1}{\alpha}}\right)$$

Parameter α can be approximate using the next relation depending on τ_{H3}:
if $0 < |\tau_{H3}| \leq 0.60$:

$$\alpha = \frac{20.52313736 - 9.9671098 \cdot |\tau_{H3}| - 1.50700583 \cdot \tau_{H3}{}^2 - 3.19977217 \cdot |\tau_{H3}|^3}{1 + 47.75141059 \cdot |\tau_{H3}|}$$

if $0.60 < |\tau_{H3}| < 0.89$:

$$\alpha = \frac{\begin{array}{c}11471.15415749 - 5766.94134229 \cdot |\tau_{H3}| - 13559.73486747 \cdot \tau_{H3}{}^2 - \\ 5023.58871075 \cdot |\tau_{H3}|^3 + 12658.21025603 \cdot \tau_{H3}{}^4\end{array}}{1 + 41914.41166725 \cdot |\tau_{H3}| - 47026.68184896 \cdot \tau_{H3}{}^2}$$

$$\beta = \frac{2 \cdot L_{H2} \cdot \alpha}{\Gamma\left(\frac{1}{\alpha}\right) \cdot \left(3^{1-\frac{1}{\alpha}} + 3 - 3 \cdot 2^{1-\frac{1}{\alpha}}\right)}$$

$$\gamma = L_{H1} + \frac{\beta}{\alpha} \cdot \Gamma\left(\frac{1}{\alpha}\right) \cdot \left(2^{-\frac{1}{\alpha}} - 2\right)$$

Appendix A.4. Generalized Pareto (GP)

For the L-moments method, the parameters are [5–7]:

$$\alpha = \frac{1 - 3 \cdot |\tau_3|}{|\tau_3| + 1}$$

$$\beta = 2 \cdot L_2 \cdot \left(1 - \frac{2 \cdot (3 \cdot |\tau_3| - 1)}{(|\tau_3| + 1)^2}\right)$$

$$\gamma = L_1 + L_2 \cdot \left(1 - \frac{4}{|\tau_3| + 1}\right)$$

For the LH-moments method, the parameters have the following expressions:

$$\alpha = \frac{4 - 12 \cdot |\tau_{H3}|}{3 \cdot |\tau_{H3}| + 4}$$

$$\beta = 2 \cdot L_{H2} \cdot \left(\frac{10 \cdot \left(33 \cdot \tau_{H3}^2 - 32 \cdot |\tau_{H3}| + 32\right)}{(3 \cdot |\tau_3| + 4)^3} - 1\right)$$

$$\gamma = \frac{40 \cdot L_{H1} \cdot (|\tau_{3H}| - 2)}{(3 \cdot |\tau_{3H}| + 4)^2} - \frac{L_{H2} - 3 \cdot L_{H1}}{3}$$

Appendix A.5. Rayleigh (RY)

For the L-moments method, the parameters are:

$$\alpha = \frac{L_2 \cdot (3 \cdot |\tau_3| - 1)}{\sqrt{\pi} \cdot \left(\sqrt{6} + \sqrt{2} - 4\right)}$$

$$\beta = L_2 - \frac{\alpha \cdot \sqrt{\pi} \cdot \left(\sqrt{2} - 1\right)}{2}$$

$$\gamma = L_1 - \frac{\alpha \cdot \sqrt{2 \cdot \pi}}{2} - 2 \cdot \beta$$

For the LH-moments method, the parameters have the following expressions:

$$\alpha = \frac{\sqrt{\pi} \cdot (12 \cdot L_{H3} - 4 \cdot L_{H2})}{\pi \cdot \left(15 \cdot \sqrt{6} - 5 \cdot \sqrt{2} - 30\right)}$$

$$\beta = \frac{4 \cdot L_{H2} \cdot \sqrt{\pi} + \alpha \cdot \pi \cdot \left(6 - 3 \cdot \sqrt{2} - \sqrt{6}\right)}{4 \cdot \sqrt{\pi}}$$

$$\gamma = \frac{\sqrt{\pi} \cdot (2 \cdot L_{H1} - 6 \cdot \beta) + \alpha \cdot \pi \cdot \left(1 - 2 \cdot \sqrt{2}\right)}{2 \cdot \sqrt{\pi}}$$

Appendix A.6. Log-Normal (LN3)

For the L- and LH-moments, the parameters are calculated using definite integrals and the inverse function.

For the L-moments, β can be approximate using the next relations depending on τ_3 [34]:
if $0 < |\tau_3| \leq \frac{1}{3}$:

$$\beta = 0.0004379498 + 2.0295824 \cdot |\tau_3| + 0.23041762 \cdot {\tau_3}^2 - 0.92166328 \cdot |\tau_3|^3 + 3.8546644 \cdot {\tau_3}^4 - 3.6560389 \cdot |\tau_3|^5$$

if $\frac{1}{3} < |\tau_3| \leq \frac{2}{3}$:

$$\beta = 0.053943247 + 2.6732827 \cdot |\tau_3| - 2.9211411 \cdot {\tau_3}^2 + 7.3388138 \cdot |\tau_3|^3 - 8.1997299 \cdot {\tau_3}^4 + 4.3299046 \cdot |\tau_3|^5$$

if $\frac{2}{3} < |\tau_3| < 1$:

$$\beta = \frac{0.81822527 + 7.818908 \cdot \tau_3^4 - 8.1529453 \cdot \tau_3^8 + 0.1554959 \cdot \tau_3^{12}}{1 + 2.5188862 \cdot \tau_3^4 - 4.9742123 \cdot \tau_3^8 + 1.592552 \cdot \tau_3^{12}}$$

The parameters α and γ are [6,7]:

$$\alpha = \ln\left(\frac{L_2}{erf(0.5)}\right) - \frac{\beta^2}{2}$$

$$\gamma = L_1 - \exp\left(\alpha + 0.5 \cdot \beta^2\right)$$

For the LH-moments method, the scale parameter β can be approximate using the next relation depending on τ_{H3}:

$$\beta = \frac{-0.299614774 + 3.042079635 \cdot |\tau_{3H}| - 2.900801018 \cdot \tau_{3H}^2}{1 - 0.933093562 \cdot |\tau_{3H}| - 0.64009136 \cdot \tau_{3H}^2 + 0.51414951 \cdot |\tau_{3H}|^3}$$

The parameters α and γ are:

$$\alpha = \ln\left(\frac{3}{2} \cdot \frac{L_{H2}}{z_1}\right)$$

$$\gamma = L_{H1} - 2 \cdot \exp(\alpha) \cdot z_2$$

where $z_1 = \int_0^1 \exp(\beta \cdot qnorm(p,0,1)) \cdot \left(3 \cdot p^2 - 2 \cdot p\right) \cdot dp$, which can be approximated with:

$$z_1 = \exp\left(\begin{array}{l} -0.4607809 + 2.1250051 \cdot \ln(\beta) + 0.863935 \cdot \ln(\beta)^2 + \\ 0.5441155 \cdot \ln(\beta)^3 + 0.3300339 \cdot \ln(\beta)^4 + 0.1507899 \cdot \ln(\beta)^5 + \\ 0.0409295 \cdot \ln(\beta)^6 + 0.0057164 \cdot \ln(\beta)^7 + 0.0003153 \cdot \ln(\beta)^8 \end{array}\right)$$

and,
$z_2 = \int_0^1 \exp(\beta \cdot qnorm(p,0,1)) \cdot p \cdot dp$, which can be approximated with:

$$z_2 = \exp\left(\begin{array}{l} 0.2270454 + 1.2930085 \cdot \ln(\beta) + 1.0189764 \cdot \ln(\beta)^2 + \\ 0.6029839 \cdot \ln(\beta)^3 + 0.3173155 \cdot \ln(\beta)^4 + 0.1468108 \cdot \ln(\beta)^5 + \\ 0.049679 \cdot \ln(\beta)^6 + 0.0104601 \cdot \ln(\beta)^7 + 0.0011938 \cdot \ln(\beta)^8 + 0.000056 \cdot \ln(\beta)^9 \end{array}\right)$$

Appendix A.7. Log-Logistic (LL3)

For the L-moments method, the parameters are [6]:

$$\alpha = \frac{1}{|\tau_3|}$$

$$\beta = \frac{L_2 \cdot \sin(|\tau_3| \cdot \pi)}{\pi \cdot \tau_3^2}$$

$$\gamma = L_1 - \frac{\beta \cdot \pi \cdot \tau_3}{\sin(|\tau_3| \cdot \pi)}$$

For the LH-moments method, the parameters are:

$$\alpha = \frac{20}{27 \cdot \tau_{H3} - 4}$$

$$\beta = \frac{4 \cdot L_{H2} \cdot \alpha \cdot \sin\left(\frac{\pi}{\alpha}\right)}{3 \cdot \pi \cdot (\alpha + 1)}$$

$$\gamma = L_{H1} - \frac{\beta \cdot \pi \cdot (\alpha + 1)}{\alpha^2 \cdot \sin\left(\frac{\pi}{\alpha}\right)}$$

References

1. Popovici, A. *Dams for Water Accumulations*; Technical Publishing House: Bucharest, Romania, 2002; Volume II.
2. *STAS 4068/1-82*; Maximum Water Discharges and Volumes, Determination of maximum Water Discharges and Volumes of Watercourses. The Romanian Standardization Institute: Bucharest, Romania, 1982.
3. Ilinca, C.; Anghel, C.G. Flood-Frequency Analysis for Dams in Romania. *Water* **2022**, *14*, 2884. [CrossRef]
4. Teodorescu, I.; Filotti, A.; Chiriac, V.; Ceausescu, V.; Florescu, A. *Water Management*; Ceres Publishing House: Bucharest, Romania, 1973.
5. Hosking, J.R.M.; Wallis, J.R. *Regional Frequency Analysis: An Approach Based on L–Moments*; Cambridge University Press: Cambridge, UK, 1997.
6. Rao, A.R.; Hamed, K.H. *Flood Frequency Analysis*; CRC Press LLC.: Boca Raton, FL, USA, 2000.
7. Singh, V.P. *Entropy-Based Parameter Estimation in Hydrology*; Springer: Dordrecht, The Netherlands, 1998.
8. Greenwood, J.A.; Landwehr, J.M.; Matalas, N.C.; Wallis, J.R. Probability Weighted Moments: Definition and Relation to Parameters of Several Distributions Expressible in Inverse Form. *Water Resour. Res.* **1979**, *15*, 1049–1054. [CrossRef]
9. Houghton, C. *Birth of a Parent: The Wakeby Distribution for Modeling Flood Flows*; Working Paper No. MIT-EL77–033WP; Water Resources Research: Tucson, AZ, USA, 1978; Volume 14.
10. Hydrology Subcommittee; Interagency Advisory Committee on Water Data; U.S. Department of the Interior; U.S. Geological Survey; Office of Water Data Coordination. *Bulletin 17B Guidelines for Determining Flood Flow Frequency; Hydrology Subcommittee; Interagency Advisory Committee on Water Data*; U.S. Department of the Interior: Reston, VA, USA; U.S. Geological Survey: Reston, VA, USA; Office of Water Data Coordination: Reston, VA, USA, 1981.
11. U.S. Department of the Interior; U.S. Geological Survey. *Bulletin 17C Guidelines for Determining Flood Flow Frequency*; U.S. Department of the Interior: Reston, VA, USA; U.S. Geological Survey: Reston, VA, USA; Office of Water Data Coordination: Reston, VA, USA, 2017.
12. Ilinca, C.; Anghel, C.G. Frequency Analysis of Extreme Events Using the Univariate Beta Family Probability Distributions. *Appl. Sci.* **2023**, *13*, 4640. [CrossRef]
13. Anghel, C.G.; Ilinca, C. Hydrological Drought Frequency Analysis in Water Management Using Univariate Distributions. *Appl. Sci.* **2023**, *13*, 3055. [CrossRef]
14. Murshed, S.; Park, B.-J.; Jeong, B.-Y.; Park, J.-S. LH-Moments of Some Distributions Useful in Hydrology. *Commun. Stat. Appl. Methods* **2009**, *16*, 647–658. [CrossRef]
15. Hosking, J.R.M. L-moments: Analysis and Estimation of Distributions using Linear, Combinations of Order Statistics. *J. R. Statist. Soc.* **1990**, *52*, 105–124. [CrossRef]
16. Wang, Q.J. LH moments for statistical analysis of extreme events. *Water Resour. Res.* **1997**, *33*, 2841–2848. [CrossRef]
17. Gaume, E. Flood frequency analysis: The Bayesian choice. *WIREs Water.* **2018**, *5*, e1290. [CrossRef]
18. Ilinca, C.; Anghel, C.G. Flood Frequency Analysis Using the Gamma Family Probability Distributions. *Water* **2023**, *15*, 1389. [CrossRef]

19. Hewa, G.A.; Wang, Q.J.; McMahon, T.A.; Nathan, R.J.; Peel, M.C. Generalized extreme value distribution fitted by LH moments for low-flow frequency analysis. *Water Resour. Res.* **2007**, *43*, W06301. [CrossRef]
20. Wang, Q.J. Approximate Goodness-of-Fit Tests of fitted generalized extreme value distributions using LH moments. *Water Resour. Res.* **1998**, *34*, 3497–3502. [CrossRef]
21. Fawad, M.; Cassalho, F.; Ren, J.; Chen, L.; Yan, T. State-of-the-Art Statistical Approaches for Estimating Flood Events. *Entropy* **2022**, *24*, 898. [CrossRef] [PubMed]
22. Lee, S.H.; Maeng, S.J. Comparison and analysis of design floods by the change in the order of LH-moment methods. *Irrig. Drain.* **2003**, *52*, 231–245. [CrossRef]
23. Ali, M.; Khalili, D. Comprehensive evaluation of regional flood frequency analysis by L- and LH-moments. II. Development of LH-moments parameters for the generalized Pareto and generalized logistic distributions. *Stoch. Environ. Res. Risk Assess.* **2009**, *23*, 137–152.
24. Ali, M.; Davar, K. Comprehensive evaluation of regional flood frequency analysis by L- and LH-moments. I. A revisit to regional homogeneity. *Stoch. Environ. Res. Risk Assess.* **2009**, *23*, 119–135. [CrossRef]
25. Abhijit, B.; Munindra, B.; Rakesh, K. Regional Flood Frequency Analysis of North-Bank of the River Brahmaputra by Using LH-Moments. *Water Resour. Manag.* **2010**, *24*, 1779–1790. [CrossRef]
26. Hossein, M.; Gheidari, N. Comparisons of the L- and LH-moments in the selection of the best distribution for regional flood frequency analysis in Lake Urmia Basin. *Civ. Eng. Environ. Syst.* **2013**, *30*, 72–84. [CrossRef]
27. Deka, S.; Borah, M.; Kakaty, S.C. Statistical analysis of annual maximum rainfall in North-East India: An application of LH-moments. *Theor. Appl. Climatol.* **2011**, *104*, 111–122. [CrossRef]
28. Zahrahtul, Z.; Jarah, S.; Mumtazimah, M. Rainfall frequency analysis using LH-moments approach: A case of Kemaman Station, Malaysia. *Int. J. Eng. Technol.* **2018**, *7*, 107–110. [CrossRef]
29. Dhruba, B.; Munindra, B.; Abhijit, B. Regional analysis of maximum rainfall using L-moment and LH-moment: A comparative case study for the northeast India. *Mausam.* **2017**, *68*, 451–462. [CrossRef]
30. Anghel, C.G.; Ilinca, C. Predicting Flood Frequency with the LH-Moments Method: A Case Study of Prigor River, Romania. *Water* **2023**, *15*, 2077. [CrossRef]
31. Diacon, C.; Serban, P. *Hydrological Syntheses and Regionalizations*; Technical Publishing House: Bucharest, Romania, 1994.
32. Ioanitoaia, R.H. *Ameliorative Hydrology*; Agro-Silvica Publishing House: Bucharest, Romania, 1962.
33. Constantinescu, M.; Golstein, M.; Haram, V.; Solomon, S. *Hydrology*; Technical Publishing House: Bucharest, Romania, 1956.
34. Chow, V.T.; Maidment, D.R.; Mays, L.W. *Applied Hydrology*; McGraw-Hill, Inc.: New York, NY, USA, 1988; ISBN 007-010810-2.
35. Crooks, G.E. *Field Guide to Continuous Probability Distributions*; Berkeley Institute for Theoretical Science: Berkeley, CA, USA, 2019.
36. Gubareva, T.S.; Gartsman, B.I. Estimating Distribution Parameters of Extreme Hydrometeorological Characteristics by L-Moment Method. *Water Resour.* **2010**, *37*, 437–445. [CrossRef]
37. Hosking, J.R.M.; Wallis, J.R. Parameter and Quantile Estimation for the Generalized Pareto Distribution. *Technometrics* **1987**, *29*, 339–349. [CrossRef]
38. Kundu, D.; Raqab, Z. Estimation of $R=P[Y<X]$ for three-parameter generalized Rayleigh distribution. *J. Stat. Comput. Simul.* **2015**, *85*, 725–739. [CrossRef]
39. Anghel, C.G.; Ilinca, C. Parameter Estimation for Some Probability Distributions Used in Hydrology. *Appl. Sci.* **2022**, *12*, 12588. [CrossRef]
40. Bîrsan, M.V. *The Variability of the Natural Flow Regime of Rivers in Romania*; Ars Docendi Publishing House: Bucharest, Romania, 2017.
41. Ministry of the Environment. *The Romanian Water Classification Atlas, Part I—Morpho-Hydrographic Data on the Surface Hydrographic Network*; Ministry of the Environment: Bucharest, Romania, 1992.
42. Yahaya, A.S.; Nor, N.M.; Jali, N.R.M.; Ramli, N.A.; Ahmad, F.; Ul-Saufie, A.Z. Determination of the Probability Plotting Position for Type I Extreme Value Distribution. *J. Appl. Sci.* **2012**, *12*, 1501–1506.
43. Ministry of Regional Development and Tourism. *The Regulations Regarding the Establishment of Maximum Flows and Volumes for the Calculation of Hydrotechnical Retention Constructions*; Indicative NP 129–2011; Ministry of Regional Development and Tourism: Bucharest, Romania, 2012.
44. Flowers-Cano, R.S.; Ortiz-Gómez, R.; León-Jiménez, J.E.; López Rivera, R.; Perera Cruz, L.A. Comparison of Bootstrap Confidence Intervals Using Monte Carlo Simulations. *Water* **2018**, *10*, 166. [CrossRef]
45. Rao, G.S.; Albassam, M.; Aslam, M. Evaluation of Bootstrap Confidence Intervals Using a New Non-Normal Process Capability Index. *Symmetry* **2019**, *11*, 484. [CrossRef]
46. Markiewicz, I.; Bogdanowicz, E.; Kochanek, K. Quantile Mixture and Probability Mixture Models in a Multi-Model Approach to Flood Frequency Analysis. *Water* **2020**, *12*, 2851. [CrossRef]
47. Kochanek, K.; Strupczewski, W.G.; Bogdanowicz, E.; Markiewicz, I. The bias of the maximum likelihood estimates of flood quantiles based solely on the largest historical records. *J. Hydrol.* **2020**, *584*, 124740. [CrossRef]
48. Markiewicz, I.; Bogdanowicz, E.; Kochanek, K. On the Uncertainty and Changeability of the Estimates of Seasonal Maximum Flows. *Water* **2020**, *12*, 704. [CrossRef]

49. Anghel, C.G.; Ilinca, C. Evaluation of Various Generalized Pareto Probability Distributions for Flood Frequency Analysis. *Water* **2023**, *15*, 1557. [CrossRef]
50. Drobot, R.; Draghia, A.F.; Chendes, V.; Sirbu, N.; Dinu, C. Consideratii privind viiturile sintetice pe Dunare. *Hidrotehnica* **2023**, *68*, 37–52. (In Romanian)